Single-Phase Direct Boost AC-AC Converter

Ovidiu URSARU, Mihai LUCANU, Cristian AGHION, Nicolae LUCANU
Gheorghe Asachi Technical University of Iasi, 700506, Romania
aghion@etti.tuiasi.ro

***Abstract*—This paper introduces and studies a boost AC-AC converter circuit that can be used to supply power to the 220V receivers in the 110V grids or to increase and adjust voltage at the end of long lines. High frequency AC-AC converters have better specifications than alternative voltage phase control drives with thyristors or TRIACs. When frequency exceeds 20kHz, noise is eliminated, filters are smaller and efficiency is higher. The current waveform is much better, the output voltage can be higher than the input voltage and voltage control is more accurate.**

***Index Terms*—power conversion, choppers, circuit simulation, pulse width modulation, power control.**

I. INTRODUCTION

AC-AC converters are used in many fields, such as AC motor drives, switching regulated AC power supplies, AC voltage waveform restorers, electric heating, lighting control, etc.

Low-frequency AC choppers are presented in [1]. References [2-4] refer to improved PWM control techniques that increase the power factor and eliminate certain harmonics. References [5,6] study a single phase AC converter with IGBTs, present improvement solutions for the chopper control technique by injecting the third harmonic into the PWM signal. In [7, 8], the three-phase AC choppers illustrated have improved specifications.

Reference [9] introduces a three-phase AC-AC converter circuit with 9 IGBTs, and [10] suggests a method for evaluating the topology of three-phase AC-AC converters. Reference [11] presents an AC-AC converter with improved specifications, submitted to simulations in order to test its operation.

A buck-boost AC chopper with improved switching is shown in [12]. Reference [13] presents a sliding control method for a single-phase buck-boost AC-AC chopper. Three-level AC-AC converters were also reported in [14] and [15]. Voltage restoration by means of an AC-AC converter with commercial modules is illustrated in [16]. References [17-19] study, analyse and design various AC-AC converters.

The paper analyses a direct boost AC-AC converter containing two inductances and four unidirectional current switches. The equations related to the operation of the circuit are deduced for the purely resistive load and for the inductive load. Simplified design equations are also presented. The adequate operation is validated both by simulation and by experimental tests. The switching frequency is 20kHz, the control circuit is simple, and the result is high efficiency and practically sinusoidal input current. The power flow can also be bidirectional, and the operation remains adequate, whatever the nature of the load.

II. CIRCUIT ANALYSIS

Fig. 1 presents a direct boost AC-AC converter circuit. Components L_f and C_f represent the input filter, L and L' are the two boost inductors, Q_1D_1 to Q_4D_4 are four unidirectional switches with FETs and diodes. The converter load contains the R_0 resistance and the L_0 inductance, and C_0 is the output capacitor. The output voltage is marked as v_0 and the load current as i_0.

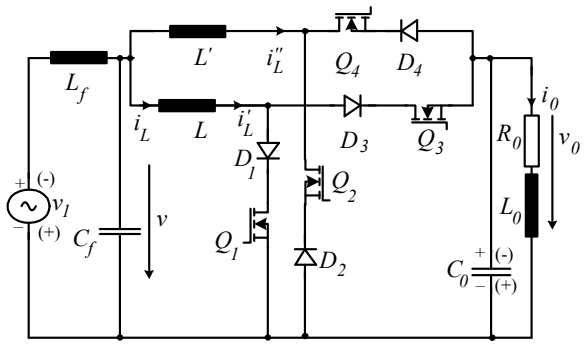

Figure 1. Direct boost AC-AC converter

Fig. 2 shows a part of the converter input voltage waveforms and the current through the boost inductance. It also presents the FETs switching diagrams. Uniform PWM control (D=const.) is used, as in the case of dc-dc converters [21]. The switching frequency is marked as $f_S=1/T_S$ and $D=t_{on}/T_S$, where t_{on} is the on time of Q_1 or Q_3 ($t_{on}=DT_S$). The switching angle $\varphi_S=\omega T_S$, where ω is the grid voltage angular frequency. Assuming that the output voltage v_0 is sinusoidal, the load impedance and the phase shift φ between voltage v_0 and current i_0 are:

$$Z=\sqrt{R_0^2+(\omega L_0)^2},\ \operatorname{tg}\varphi=\frac{\omega L_0}{R_0} \tag{1}$$

A. The resistive load case

The equivalent circuits are based on the following simplifying hypotheses: the passive components and the switches are ideal and the voltage v is sinusoidal ($v=\sqrt{2}V\sin\omega t$). We shall derive the equations for the positive half cycle of the grid voltage.

Fig. 3 presents equivalent circuits corresponding to a switching period. For the interval $t\in[0,DT]$, the equivalent circuit is represented in Fig. 3a.

Considering that k^{th} is the switching period in which:

$$t\in[t_{k-1},t_k],\ t_k=kT_S,\ t_0=0. \tag{2}$$

Digital Object Identifier 10.4316/AECE.2017.04006

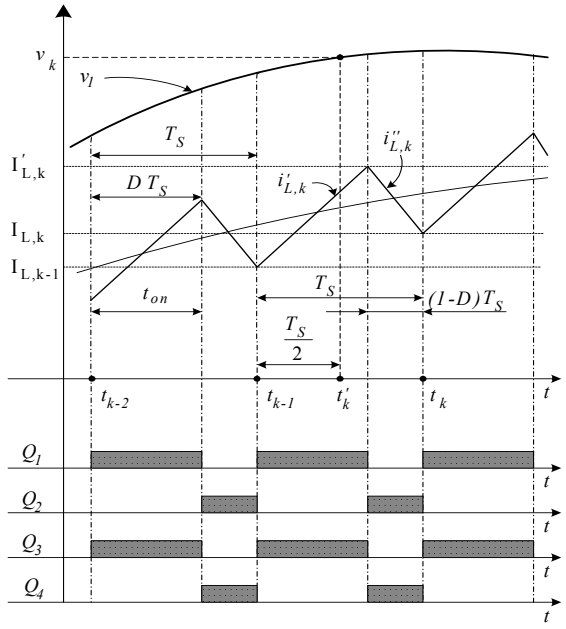

Figure 2. Waveforms of the input converter voltage *v*, boost inductor current i_L and switches conduction areas

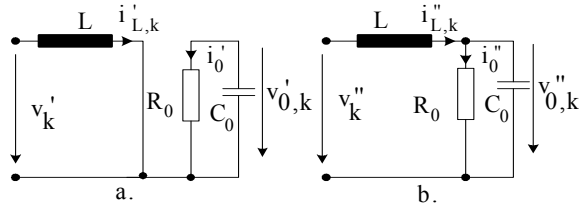

Figure 3. Equivalent circuits for the resistive load case in a switching period k in the positive half-cycle of the grid a) $t \in [0, DT]$ and b) $t \in [0,(1-D)T_S]$

marking with m_f the frequency modulation ratio:

$$m_f = \frac{f_S}{f} = \frac{2\pi}{\omega T_S} = \frac{2\pi}{\varphi_S} \quad k = \overline{1,m} \tag{3}$$

with the time origin in t_{k-1} , the input voltage equation is:

$$v'_k = \sqrt{2}V \sin(\omega t + \omega t_{k-1}) = \sqrt{2}V \sin[\omega t + (k-1)\varphi_S] \tag{4}$$

The current through the inductor *L*, i'_L, results from the following equation:

$$L\frac{d'i_{L,k}(t)}{dt} = \sqrt{2}V \sin[\omega t + (k-1)\varphi_S] \tag{5}$$

Here is the solution of this equation based on the initial condition $i'_{L,k}(0) = I_{L,k-1}$ (Fig. 2):

$$i'_{L,k}(t) = \frac{\sqrt{2}V}{\omega L}\{\cos(k-1)\varphi_S - \cos[\omega t + (k-1)\varphi_S]\} + I_{L,k-1} \tag{6}$$

Taking into account that $t=DT_S$, $\omega t=D\varphi_S$, this equation leads to:

$$I'_{L,k} = I_{L,k-1} + \frac{\sqrt{2}V}{\omega L}\{\cos(k-1)\varphi_S - \cos[D\varphi_S - (k-1)\varphi_S] = I_{L,k-1} + \frac{2\sqrt{2}V}{\omega L}\sin\frac{D\varphi_S}{2}\sin(2k-2+D)\frac{\varphi_S}{2} \tag{7}$$

In the load circuit, C_0 discharges on R_0 , therefore:

$$v'_{0,k}(t) = V_{0,k-1}e^{-\frac{t}{R_0C_0}} \tag{8}$$

$V_{0,k-1}$ is the output voltage at the moment t_{k-1}. When replacing in (8) $t=DT_S$, we get:

$$V'_{0,k} = V_{0,k-1}e^{-\frac{DT_S}{R_0C_0}} \tag{9}$$

For the second interval $t \in [0,(1-D)T_S]$, the corresponding circuit is shown in Fig. 3b. With the time origin in t_k+DT_S, $v''_k(t) = \sqrt{2}V \sin[\omega t + (k-1+D)\varphi_S]$, the resulting equation is presented below:

$$i''_{L,k}(t) = \frac{v''_{0k}(t)}{R_0} + C_0\frac{dv''_{0k}(t)}{dt} \tag{10}$$

and it leads to :

$$\frac{d^2v''_{0k}(t)}{dt^2} + \frac{1}{R_0C_0}\frac{dv''_{0k}(t)}{dt} + \frac{1}{LC}v''_{0k}(t) = = \frac{\sqrt{2}V}{LC}\sin[\omega t + (k-1+D)\varphi k] \tag{11}$$

It should be integrated into the initial conditions:

$$v''_{0k}(0) = V'_{0k};\ \frac{dv''_{0k}(0)}{dt} = \frac{1}{C}I'_{Lk} - \frac{1}{RC}V'_{0k} \tag{12}$$

The solution of the equation is the following:

$$v''_{0k}(t) = A_1\sin[\omega t + e^{-\delta t}(A_3\sin\omega' t + A_4\cos\omega' t) + (k-1+ +(+D)\varphi_S] + e^{-\delta t}(A_3\sin\omega' t + A_4\cos\omega' t) \tag{13}$$

where:

$$\begin{cases} A_1 = \dfrac{\sqrt{2}V}{1-\left(\dfrac{\omega L}{R_0}\right)^2\left[(\omega R_0C_0)^2-1\right]} \\ A_2 = \dfrac{\sqrt{2}V\dfrac{\omega L}{R_0}(\omega R_0C_0-1)}{1-\left(\dfrac{\omega L}{R_0}\right)^2[(\omega R_0C_0)^2-1]} \\ \delta = \dfrac{1}{2R_0C_0},\ \omega' = \sqrt{\dfrac{1}{LC_0} - \dfrac{1}{4R_0^2C_0^2}} \end{cases} \tag{14}$$

$$\begin{cases} A_3 = \dfrac{I'_{L,k}}{C_0\omega'} - \dfrac{V'_{0,k}}{2R_0C_0\omega'} - \left(A_1\dfrac{\omega}{\omega'} + A_2\dfrac{\delta}{\omega'}\right)\cos(k-1+D)\varphi_S \\ -\left(A_1\dfrac{\delta}{\omega'} - A_2\dfrac{\omega}{\omega'}\right)\sin(k-1+D)\varphi_S \\ A_4 = V'_{0k} - A_1\sin(k-1+D)\varphi_S - A_2\cos(k-1+D)\varphi_S \end{cases} \tag{15}$$

By replacing (14) in (11), we get:

$$i''_{L,k}(t) = \left(\frac{A_1}{R_0} - A_2C_0\omega\right)\sin\left[\omega t + (k-1+D)\varphi_S\right] + \left(\frac{A_2}{R_0} + A_1C_0\omega\right)\cos\left[\omega t + (k-1+D)\varphi_S\right] + e^{-\delta t}\left\{\left[\frac{A_3}{R_0} - C_0(\delta A_3 + \omega' A_4)\right]\sin\omega' t + \left[\frac{A_4}{R_0} - C_0(\delta A_4 - \omega' A_3)\right]\cos\omega' t\right\} \tag{16}$$

When we adjust equations (13) and (16) for $t=(1-D)T_S$

we get the output voltage and the current through the inductor L at the end of the switching period k:

$$V_{0K} = A_1 \sin k\varphi_S + A_2 \cos k\varphi_S + e^{-\frac{\delta}{\omega}(1-D)\varphi_S} \cdot \left\{ A_3 \sin\left[\frac{\omega'}{\omega}(1-D)\varphi_S\right] + A_4 \cos\left[\frac{\omega'}{\omega}(1-D)\varphi_S\right]\right\} \quad (17)$$

$$I_{LK} = \left(\frac{A_1}{R_0} - A_2 C_0 \omega\right)\sin k\varphi_S + \left(\frac{A_2}{R_0} + A_1 C_0 \omega\right)\cdot \cos k\varphi_S + e^{-\frac{\delta}{\omega}(1-D)\varphi_S}\cdot\left\{\left[\frac{A_3}{R_0} - C_0\left(\delta A_3 + \omega' A_4\right)\right]\cdot \sin\left[\frac{\omega'}{\omega}(1-D)\varphi_S\right] + \left[\frac{A_4}{R_0} - C_0\left(\delta A_4 - \omega' A_3\right)\right] + \cos\left[\frac{\omega'}{\omega}(1-D)\varphi_S\right]\right\} \quad (18)$$

B. The inductive load case

In the inductive load case, we shall consider the simplifying hypothesis that, due to the load, the current is practically constant, leading to the equivalent circuits in Fig. 4. For the interval $t \in [0, DT]$, the equivalent circuit is represented in Fig. 4.a. At this point, we consider the switching period k when $t \in [t_{k-1}, t_k]$.

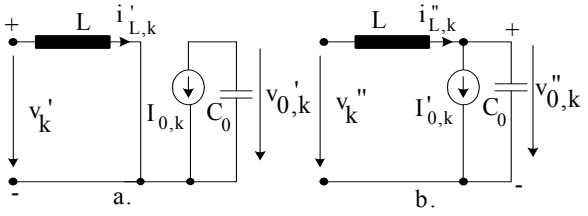

Figure 4. Equivalent circuits for the inductive load case in a switching period k^{th} in the positive half-cycle of the grid a) $t \in [0, DT_S]$ and b) $t \in [0, (1-D)T_S]$

Since the inductor is connected as in Fig. 3.a., the equation of the current flowing through it is equation (6), and at the end of the interval, the current value will result from equation (7). In the load circuit, the capacitor C_0 discharges under the constant current $I_{0,k-1}$ generated at the end of the previous switching period. Therefore:

$$v'_0(t) = V_{0,k-1} - \frac{I_{0,k-1}\cdot t}{C_0} \quad (19)$$

at the end of the conduction interval $t=DT_S$. Here are the resulting equations:

$$V'_{0,k} = V_{0,k-1} - \frac{D\varphi_S I_{0,k-1}}{\omega C_0} \quad (20)$$

$$I'_{0,k} \approx \frac{V'_{0,k}}{R_0} = \frac{V_{0,k-1}}{R_0} - \frac{D\varphi_S I_{0,k-1}}{\omega R_0 C_0} \quad (21)$$

In these equations, $V_{0,k-1}$ is the output voltage at the end of the switching period *k-1*.

For the second conduction interval, $t \in [0, (1-D)T_S]$ the equivalent circuit is represented in Fig. 4b, and the corresponding equations are presented below:

$$L\frac{di"_{L,k}}{dt} + v"_{0,k}(t) = v"_k(t) \quad (22)$$

$$i"_{L,k}(t) = I'_{0,k} + C_0\frac{dv"_{0,k}(t)}{dt} \quad (23)$$

In these equations $v"_{0,k}(t) = \sqrt{2}V\sin\left[\omega t + (k-1+D)\varphi_S\right]$

The resulting differential equation:

$$\frac{d^2 v"_{0,k}(t)}{dt^2} + \frac{1}{LC_0}v"_{0,k}(t) = = \frac{\sqrt{2}V}{LC_0}\sin\left[\omega t + (k-1+D)\varphi_S\right] \quad (24)$$

must be solved taking into account the initial conditions:

$$v"_{0,k}(0) = V'_{0,k},$$

$$\frac{dv"_{0,k}(0)}{dt} = \frac{1}{C_0}\left(I'_{L,k} - I'_{0,k}\right) = = \frac{1}{C_0}\left(I'_{L,k} - \frac{V_{0,k-1}}{R_0} + \frac{D\varphi_S I_{0,k-1}}{\omega R_0 C_0}\right) \quad (25)$$

Here is the solution:

$$v"_{0,k}(t) = \frac{\sqrt{2}V}{1-\omega^2 LC_0}\sin\left[\omega t + (k-1+D)\varphi_S\right] + + B_1\sin\frac{t}{\sqrt{LC_0}} + B_2\cos\frac{t}{\sqrt{LC_0}} \quad (26)$$

The integration constants B_1 and B_2 are:

$$\begin{cases} B_1 = \left(I'_{L,k} - I'_{0,k}\right)\sqrt{\frac{L}{C_0}} - \frac{\sqrt{2}V\omega\sqrt{LC_0}}{1-\omega^2 LC_0}\cdot \\ \cdot\cos\left[(k-1+D)\varphi_S\right] \\ B_2 = V'_{0,k} - \frac{\sqrt{2}V}{1-\omega^2 LC_0}\sin\left[(k-1+D)\varphi_S\right] \end{cases} \quad (27)$$

The current through the inductor L will result from the equation:

$$i"_{L,k}(t) = I'_{0,k} + \frac{\sqrt{2}\omega VC_0}{1-\omega^2 LC_0}\cos\left[\omega t + (k-1+D)\varphi_S\right] + + B_1\sqrt{\frac{C_0}{L}}\cos\frac{t}{\sqrt{LC_0}} - B_2\sqrt{\frac{C_0}{L}}\sin\frac{t}{\sqrt{LC_0}} \quad (28)$$

When $t = (1-D)T_S$, $\omega t = (1-D)\varphi_S$, equations (26) and (28) become:

$$I_{L,k} = I'_{0,k} + \frac{\sqrt{2}\omega VC_0}{1-\omega^2 LC_0}\sin(k\varphi_S) + + B_1\sqrt{\frac{C_0}{L}}\cos\left[\frac{(1-D)\varphi_S}{\omega\sqrt{LC_0}}\right] - B_2\sqrt{\frac{C_0}{L}}\sin\left[\frac{(1-D)\varphi_S}{\omega\sqrt{LC_0}}\right] \quad (29)$$

$$V_{0,k} = \frac{\sqrt{2}V}{1-\omega^2 LC_0}\sin(k\varphi_S) + + B_1\sin\left[\frac{(1-D)\varphi_S}{\omega\sqrt{LC_0}}\right] + B_2\cos\left[\frac{(1-D)\varphi_S}{\omega\sqrt{LC_0}}\right] \quad (30)$$

$$I_{0,k} \approx \frac{1}{R_0}V_{0,k} \quad (31)$$

These equations show the current through the inductor L, as well as the voltage and the load current at the end of the switching period K, taking into account the same values registered at the beginning of this period.

C. SIMPLIFIED CONVERTER EQUATIONS

The equations presented above are complex and hard to work with. We can obtain comparative simpler equations that can be used in design calculations if we assume that, in a switching period, the input and output voltages of the converter are constant. For the analysis of the switching period *k*, we use the equivalent circuits in Fig. 5.

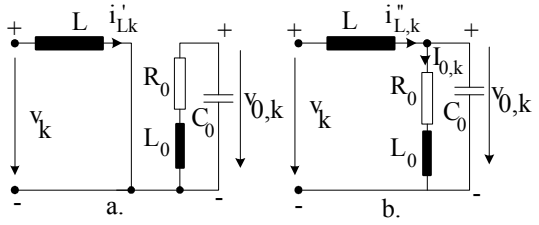

Figure 5. Equivalent circuits for a switching period k^{th}, in the positive half cycle of the network, used for the simplified analysis a) $t \in [0, DT_S]$ and b) $t \in [0,(1-D)T_S]$

$$\begin{cases} v_k = \sqrt{2}V \sin \omega t'_k \\ t'_k = (k-1)T_S + \dfrac{T_S}{2} \end{cases} \quad (32)$$

Since it is a boost converter, the constant output voltage is:

$$V_{0,k} = \frac{\sqrt{2}V}{1-D}\sin \omega t'_k, \; I_{0,k} = \frac{\sqrt{2}V}{R_0(1-D)}\sin \omega t'_k \quad (33)$$

a) For the time interval $t \in [0, DT_S]$, the equivalent circuit is presented in Fig. 5a. In the positive half cycle, the current $i'_{L,k}$ will flow through Q_1. The average current and the maximum repetitive current are shown in ([18] p. 96):

$$I_{Q1,kAVR} = I_{D1,k\,AVR} = \frac{\sqrt{2}DV \sin \omega t'_k}{R_0(1-D)^2} \quad (34)$$

$$I_{Q1,k\,RM} = I_{D1,k\,RM} = \frac{\sqrt{2}V \sin \omega t'_k}{R_0(1-D)^2} + \frac{\sqrt{2}DV \sin \omega t'_k}{2Lf_S} \quad (35)$$

b) For the time interval $t \in [0,(1-D)T_S]$, the equivalent circuit is represented in Fig. 5b. The current $i''_{L,k}$ will flow through D_2 and Q_2. The average and maximal repetitive currents are:

$$I_{Q2,k\,AVR} = I_{D2,k\,AVR} = \frac{\sqrt{2}V \sin \omega t'_k}{R_0(1-D)} \quad (36)$$

$$I_{Q2,k\,RM} = I_{D2,k\,RM} = \frac{\sqrt{2}V \sin \omega t'_k}{R_0(1-D)^2} + \frac{\sqrt{2}DV \sin \omega t'_k}{2Lf_S} \quad (37)$$

In the negative half-cycle, the currents will flow through D_3, Q_3 and D_4, Q_4 respectively, and the same equations apply. Given that all switches are in conduction only in a half-period of the a.c. grid voltage, the average and maximal repetitive currents through diodes and transistors are calculated by means of the equations below:

$$I_{Q1\,AVR} = I_{Q3\,AVR} = I_{D1\,AVR} = I_{D3\,AVR} = \frac{\sqrt{2}DV}{\pi R_0(1-D)^2} \quad (38)$$

$$I_{Q2\,AVR} = I_{Q4\,AVR} = I_{D2\,AVR} = I_{D4\,AVR} = \frac{\sqrt{2}V}{\pi R_0(1-D)} \quad (39)$$

For all components:

$$I_{Q\,RM} = I_{D\,RM} = \frac{\sqrt{2}V}{R_0(1-D)^2} + \frac{\sqrt{2}DV}{2Lf_S} \quad (40)$$

The voltage stress of the components is:

$$V_{RM} = \frac{\sqrt{2}V}{1-D} \quad (41)$$

III. SIMULATION AND EXPERIMENTAL TESTS

The adequate operation of the circuit was tested by simulation and experimental prototype. The load used in the simulations and in the prototype is the same, i.e. a resistive load: $R = 150\ \Omega$ and an inductive load: $L = 32\ mH$.

The components of the simulated circuit have the following values: the grid filter [20] is made up of L_f=*4mH*, C_f=*10uF*, the boost inductances $L = L' = 0.2\ mH$. The amplitude of the grid voltage is *155V* and the switching frequency is $f = 20KHz$.

The simulations took into account the following values of the duty cycle: *D=0.2, 0.4*, and *0.6*. The paper presents only some of the waveforms obtained, namely the most representative ones. Thus, Figure 6 shows the waveforms of the v_m grid voltage and of the v_0 load voltage, as well as the waveforms of the i_m current supplied by the grid and the i_0 load current for *D=0.2*.

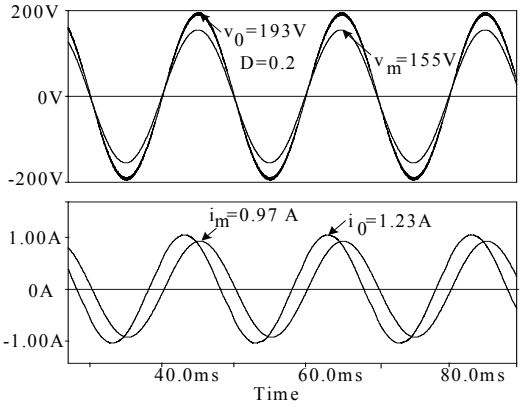

Figure 6. Waveforms of the v_m voltage, v_0 voltage, i_m current and i_0 current, for D=0.2

Figure 7 presents the same waveforms for D=0.4.

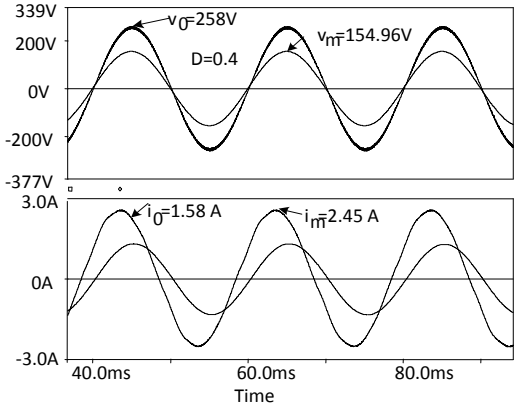

Figure 7. Waveforms of the v_m voltage, v_0 voltage, i_m current and i_0 current, for D=0.4

Figure 8 presents the same waveforms for D=0.6 . The waveforms of the load voltage and current are nearly sinusoidal.

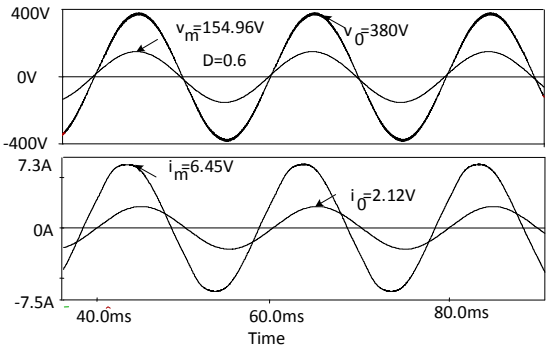

Figure 8. Waveforms of the v_m voltage, v_0 voltage, i_m current and i_0 current, for D=0.6

The laboratory prototype presented in Figure 9 was built and tested with the following parameters: input voltage $V_m = 110\ V$ and $f_m = 50Hz$. The components of the power supply filter are: $L_f=4mH$, $C_f=10\mu F$ and the switching frequency is $f=20\ kHz$.

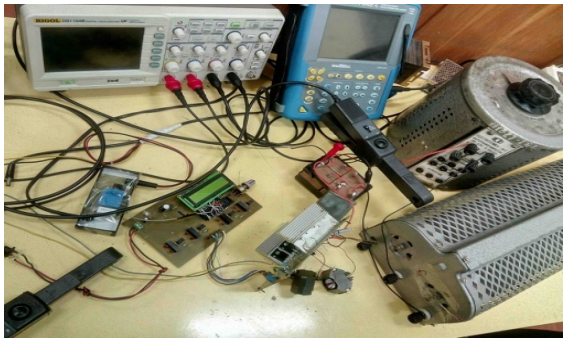

Figure 9. Experimental setup contains: control circuit, boost converter, load inductor and load resistor

Figure 10(a) shows the waveforms of the v_o voltage and of the v_m voltage and Figure 10(b) shows the waveforms of the i_o current and of the i_m current for a duty factor $D=0.2$.

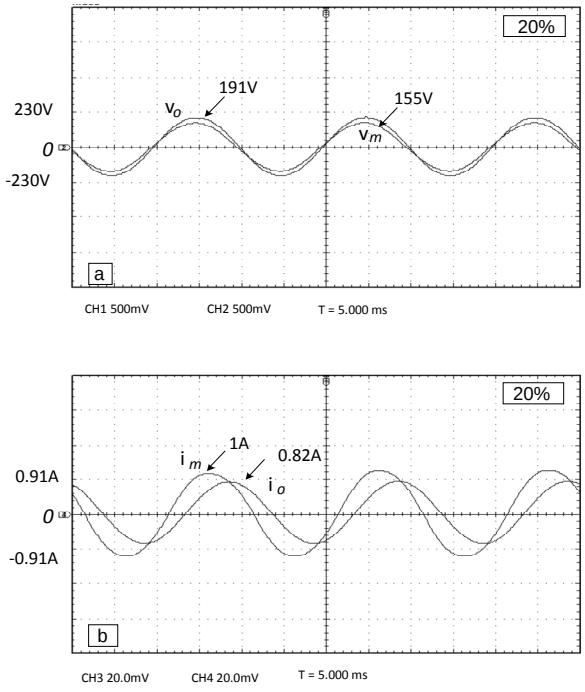

Figure 10. a)Waveforms of the v_o voltage, v_m voltage; b) Waveforms of the i_o current, and i_m current for $D=0.2$

Figure 11(a), 11(b) and Figure 12(a), 12(b) respectively, show the same waveforms for $D=0.4$ and $D=0.6$.

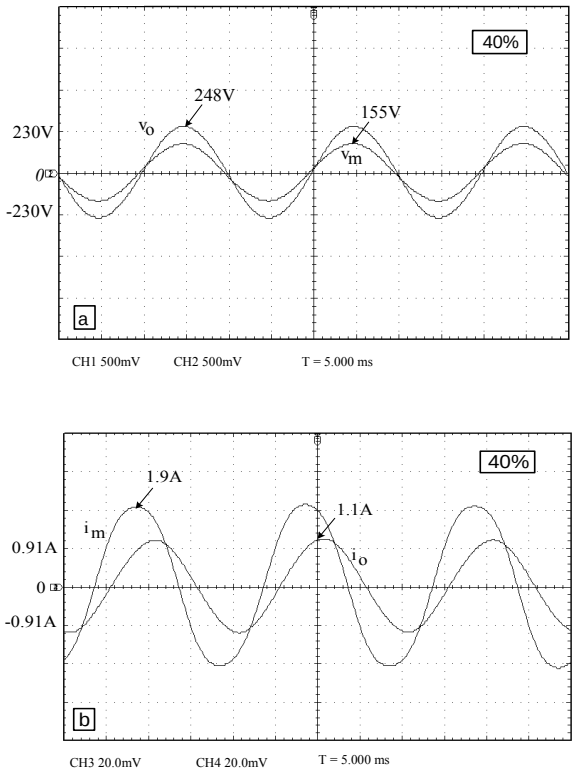

Figure 11. a)Waveforms of the *vo* voltage, *vm* voltage; b) Waveforms of the *io* current, and *im* current for D=0.4

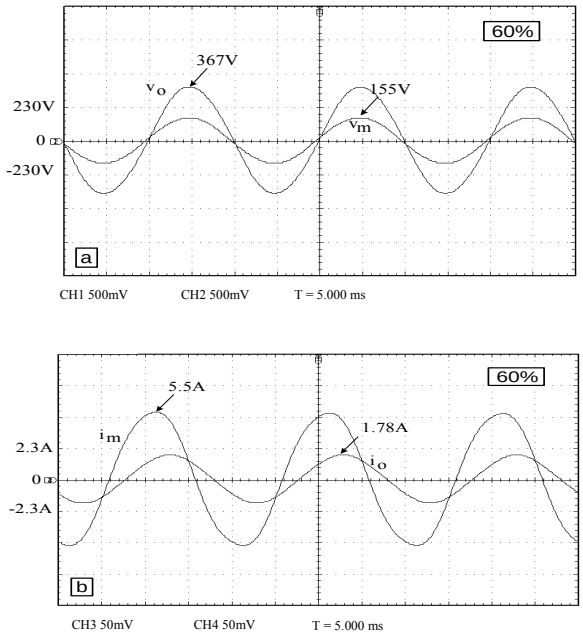

Figure 12. a)Waveforms of the *vo* voltage, *vm* voltage; b) Waveforms of the *io* current, and *im* current for D=0.6

Figure 13 shows the variations of the efficiency depending on the duty cycle D, also based on the simulation results. We notice thus that the efficiency is high for all the values of D.

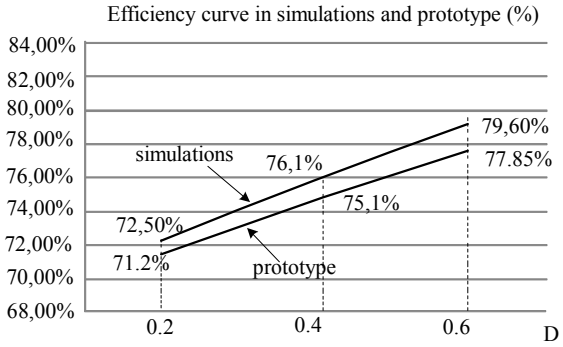

Figure 13. Variation of the efficiency depending on the duty cycle *D*.

For calculating the THD and Power Factor, the following equations were used:

$$THD = \frac{\sqrt{I_{02}^2 + I_{03}^2 + I_{04}^2}}{I_{01}}, \quad PF = \frac{1}{\sqrt{1 + THD_i^2}} \cos\varphi \qquad (42)$$

where I_{01} is the RMS value of the input current fundamental, I_{02} is the RMS value of the first harmonic of the input current at a switching frequency of 20KHz, etc.

Figure 14 compares (simulation vs. prototype) the THD and PF analyses of the current supplied by the power source, for the inductive load case.

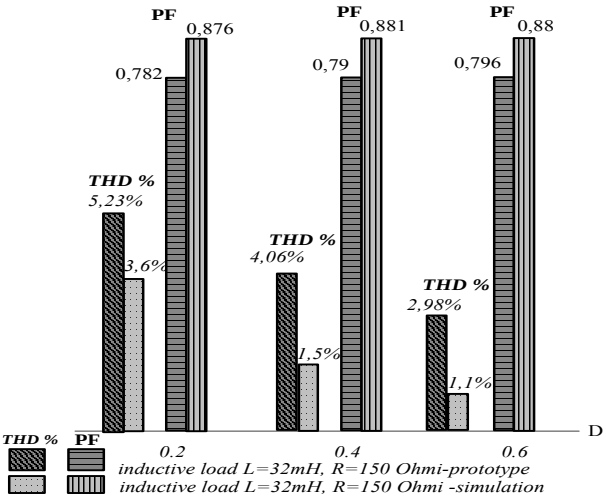

Figure 14. THD and PF analysis for the input current for the inductive load

IV. Conclusion

This paper presents the analysis, simulation and practical design of a boost AC-AC converter integrating fours switches controlled simultaneously two by two, independent of the input voltage alternation. We demonstrated the adequate operation of the circuit by simulation and by practical design for various values of the control factor of the MOS transistors used as switches. We noted the variation characteristic of the converter energetic efficiency for the various values of the control factor (D=0.2, 0.4 and 0.6), both by simulation and for the practical circuit.

Although the AC-AC converter circuit analysed illustrates the single-phase scenario, it can be easily adapted for three-phase systems.

References

[1] G. N. Revenkar, D. S. Trasi, "Symmetrical pulse width modulated a. c. chopper," I.E.E.E. Trans. on Ind. Electron. Contr. Instrum., vol. IECI-24, pp. 41 – 45, 1977. doi: 10.1109/TIECI.1977.351439

[2] G. Chose, M. Park, "An improved pwm technique for a.c. chopper," I.E.E.E. Trans. on Power Electronics, vol 4, pp. 496 – 505, 1989. doi: 10.1109/63.41778

[3] D. Jang, G. Choe, "Asymmetrical pwm method for a.c. chopper with improved input power factor," I.E.E.E. PESC Conf. Rec, 1991, pp. 838 - 845. doi: 10.1109/PESC.1991.162773

[4] Jang Do-Hyum, Ghy-Ha Choe, M. Ehsany, "Asymmetrical pwm technique with harmonic elimination and power factor control in a.c. chopper," I.E.E.E. Trans. on Power Electron., vol. 10, No. 2, pp.175-184, March 1995. doi: 10.1109/63.372602

[5] M. Lucanu, O.Ursaru, C. Aghion, "Single phase a.c. choppers with I.G.B.T's," Proceedings of the International Symposium on Signal, Circuits and Systems SCS 2003, July 10-11, 2003, pp. 213 - 216. doi: 10.1109/SCS.2003.1226986

[6] M. Derick, P. A. Athira, M. Bincy, "Modified Single Stage AC-AC Converter", International Journal of Power Electronics and Drive System (IJPEDS), vol. 6, No. 1, pp. 1-9, 2015 DOI: http://dx.doi.org/10.11591/ijpeds.v6.i1.pp1-9

[7] O.Ursaru, M. Lucanu, C. Aghion, L. Tigaeru,"Three-phase ac chopper with I.G.B.T's,with the load connected in star shape with ground wire," Buletinul Institutului Politehnic Iasi, tomul L(LIV), fasc.1-2/2004, pp.87-97.

[8] O.Ursaru, M. Lucanu, C. Aghion, L. Tigaeru,"Three-phase ac chopper with I.G.B.T's," International Conference on Development and Application Systems, May 2004, Suceava, pp.87-97, ISBN973-666-106.

[9] L. Congwei, W. Bin, N. R. Zargari, X. Devei, and W. Jiacheng, "A novel three-phase three leg AC/AC converter using nine IGBT's," I.E.E.E. Trans. on Power Electron., vol. 24, No. 5, pp. 1151 – 1160, May 2009. doi: 10.1109/TPEL.2008.2004038

[10] R. Lai, F. Wang, R. Burgos, Y. Pei, D. Boroyevich, B.Wang, T. A. Lipo, V. D. Immanuel, K. J. Karimi, "A systematic topology evaluation methodology for high-density three-phase PWM AC-AC converters," I.E.E.E. Trans. on Power Electron., vol. 24, No. 7, pp. 1671 – 1681, July 2009. doi: 10.1109/TPEL.2008.2005381

[11] M. Lucanu, O.Ursaru, C. Aghion, "Single phase a.c. choppers with inductive load and improved efficiency," Proceedings of the International Symposium on Signal, Circuits and Systems, ISSCS 2005, vol. 2, pp. 597 – 600, July 14-15 2005. doi: 10.1109/ISSCS.2005.1511311

[12] J. H. Kim, B. D. Min, B. H. Kwon, S. C. Won, "A PWM buck-boost AC chopper solving the commutation problem," I.E.E.E. Trans. on Ind. Electron., vol 45, No. 5, pp. 832 – 835, 1998. doi: 10.1109/41.720341

[13] L. Garcia de Vicuna, M. Castilla, J. Miret, J. Matas, J. M. Guerrero, "Sliding mode control for a single-phase ac/ac quantum resonant converter," I.E.E.E. Trans. on Ind. Electron., vol 56, No. 6, pp. 3496 – 3504, Sept. 2009. doi: 10.1109/TIE.2009.2026766

[14] J. Yang, L. Li, K. Yang, "Buck-boost mode single stage three level ac/ac converter," I.E.E.E. Indus. Electro. (IECON), pp. 596 – 600, 2008. DOI: 10.1109/IECON.2008.4758021

[15] L. Li, Y. Yang, Q. Zhong, "Novel family of single-stage three level a.c. choppers," I.E.E.E. Trans. on Power Electron., vol. 26, No. 2, pp. 504 – 511, 2001. doi: 10.1109/TPEL.2010.2061866

[16] Thiago B. Soliero, Clovis A. Petry, Joao C. dos S. Fagundes, Yvo Barbi, "Direct ac-ac converters using commercial power modules applied to voltage restorers," I.E.E.E. Trans. on Ind. Electron., vol 58, No. 1, pp. 278 – 288, 2011. doi: 10.1109/TIE.2010.2045320

[17] F. Yalcin, F. A Himmelstoss, "A New Transformerless Single-Phase Buck-Boost AC Voltage Regulator", Advanced in Electrical and Computer Engineering Jurnal-Suceava, vol.16, No. 2, pp. 63 – 68, 2016, DOI: 10.4316/AECE.2016.02009

[18] M. Lucanu, O.Ursaru, C. Aghion, N. Lucanu,"Single phase direct ac-ac step-down converter," IET Power Electronics, vol.7, Issue12, pp. 3101-3109, 2014. doi: 10.1049/iet-pel.2013.0730

[19] F. A. Himmelstoss, A. R Derin, M. Cernat, "Boost Converter with Active Snubber", Advanced in Electrical and Computer Engineering Jurnal-Suceava, vol. 17, No. 1, pp. 55 – 60, 2017, DOI: 10.4316/AECE.2017.01008

[20] G. Rata, M. Rata, I. Graur, D.L. Milici, "Induction Motor Speed Estimator Using Rotor Slot Harmonics", Advanced in Electrical and Computer Engineering Jurnal-Suceava, vol.9, No. 1, pp. 70-73, 2009. doi: 10.4316/AECE.2009.01013